RSC Advances

This is an *Accepted Manuscript*, which has been through the Royal Society of Chemistry peer review process and has been accepted for publication.

Accepted Manuscripts are published online shortly after acceptance, before technical editing, formatting and proof reading. Using this free service, authors can make their results available to the community, in citable form, before we publish the edited article. This *Accepted Manuscript* will be replaced by the edited, formatted and paginated article as soon as this is available.

You can find more information about *Accepted Manuscripts* in the Information for Authors.

Please note that technical editing may introduce minor changes to the text and/or graphics, which may alter content. The journal's standard Terms & Conditions and the Ethical guidelines still apply. In no event shall the Royal Society of Chemistry be held responsible for any errors or omissions in this *Accepted Manuscript* or any consequences arising from the use of any information it contains.

ROYAL SOCIETY OF CHEMISTRY

www.rsc.org/advances

Sol-Gel Entrapped Visible Light Photocatalysts for Selective Conversions

Yanhui Zhang,[a] **Rosaria Ciriminna**,[b] **Giovanni Palmisano**,[c] **Yi-Jun Xu**,*[a] **Mario Pagliaro***[b]

[a]*State Key Laboratory of Photocatalysis on Energy and Environment, College of Chemistry and Chemical Engineering, Fuzhou University, Fuzhou 350002, P.R. China;* [b]*Istituto per lo Studio dei Materiali Nanostrutturati, CNR, via U. La Malfa 153, 90146 Palermo, Italy;* [c]*Dipartimento di Fisica e Chimica, Università degli Studi di Palermo, viale delle Scienze, 90128 Palermo, Italy*

Abstract: A general method to heterogenize, stabilize and significantly enhance the activity of selective visible light photocatalysts for aerobic oxidation of glycerol is devised. The new method makes use of the sol-gel encapsulation of photocatalytic species in silica-based matrices to afford leach-proof catalysts capable to afford valued products at low cost with little or no waste generation. In particular, the photocatalytic selective conversion of glycerol is performed in water solvent at ambient conditions with molecular oxygen as oxidant and visible light as the driving energy source, thereby meeting all requirements for a green chemical process. Entrapment of the semiconductor-based photocatalyst inside the transparent porous silica matrix enhances substrate adsorption, thus improving its local concentration and favoring reaction with the photogenerated active species.

Keywords: visible light photocatalyst; sol-gel; selective oxidation; encapsulation; bismuth wolframate

**Corresponding Authors*

Dr Mario Pagliaro
Istituto per lo Studio dei Materiali Nanostrutturati, CNR
via U. La Malfa 153, 90146 Palermo (Italy)
mario.pagliaro@cnr.it

Prof. Yi-Jun Xu
State Key Laboratory of Photocatalysis on Energy and Environment, College of Chemistry and Chemical Engineering, Fuzhou University, Fuzhou, 350002 (P.R. China)
yjxu@fzu.edu.cn

RSC Advances Accepted Manuscript

Semiconductor-based photocatalysis, especially using the semiconductor TiO_2, is generally a non-selective process suitable for degradation of organics, rather than for organic synthesis,[1] even though some progress towards more selective photosynthetic processes using modified titania has been achieved.[2] Further progress on semiconductor-based photocatalysis highlights that the appropriate choice of semiconductors (*e.g.,* tuning the structure, morphology and interface composition) and optimization of reaction parameters are able to promote the occurrence of photocatalytic organic synthesis with high selectivity.[3]

Recently, in the context of this progress, flower-like Bi_2WO_6 has been identified as a highly selective visible light photocatalyst toward aerobic selective oxidation of glycerol to dihydroxyacetone (DHA),[4] using oxygen as oxidant in water at room temperature and atmospheric pressure. Besides meeting all requirements for a truly green chemical process, the method suggests the promising potential applications of semiconductor Bi_2WO_6-based photocatalysis in the field of biomass conversion to value-added fine chemicals under mild conditions.[3,5]

Sol-gel silica is transparent to both visible and UV light radiation, and the sol-gel encapsulation is known to chemically and physically stabilize the entrapped species.[6,6] Such a heterogenization strategy via so-gel silica encapsulation provides a tunable control of microscopically confined environment surrounding the entrapped photoactive species, thereby tuning the efficiency and selectivity of photocatalytic processes.[7,8] Hence, in principle, entrapment of photocatalysts in transparent SiO_2 glasses might be desirable to stabilize, recover and reuse the entrapped photocatalyst. In particular, the entrapment within sol-gel silica can largely increase the surface area of catalyst, which would increase the adsorption capacity of catalyst toward reactant inside the sol-gel silica cages that consequently could contribute to the enhanced photoactivity. Yet, so far, only a few reports exist concerning sol-gel entrapped photocatalysts, even if a broad photochemistry of sol-gel doped glasses has been developed since the late 1980s.[7]

Two typical examples of entrapped photocatalysts are sodium decatungstate supported on sol-gel silica employed in the oxidation of glycerol under UV light irradiation;[8] and silica-entrapped $H_4SiW_{12}O_{40}$ UV light photocatalyst used for the aerobic oxidation of various primary and secondary benzylic alcohols into the corresponding carbonyl compounds.[9] However, to the best of our knowledge, no encapsulation of *visible light* photocatalyst has been previously reported for selective oxidation of glycerol. To develop highly photoactive visible-light-driven semiconductor-based photocatalyst is far more desirable than that of UV light photocatalyst, from a viewpoint of efficient and sustainable use of solar energy for practical applications. Herein, we report a simple and feasible method to directly transform flower-like Bi_2WO_6 into an entrapped sol-gel catalyst with enhanced photoactivity, retaining the high selectivity. The resulting silica-entrapped Bi_2WO_6 can be used as visible light photocatalyst for the aerobic selective conversion of glycerol to related products, such as dihydroxyacetone and glyceraldehyde, in water under ambient conditions. The as-obtained results are not trivial because reactivity, compared to the non-entrapped photocatalyst, in general is altered and can be greatly enhanced.

Data in Table 1 show that the two silica-entrapped Bi_2WO_6 catalysts are highly active, despite with remarkable differences in selectivity. Results are indeed impressive because now 8 mg of entrapped catalyst are enough to catalyze the reaction at noticeable extent. We are dealing indeed with 8 mg of silica-entrapped catalysts whose content of visible-light-photoactive bismuth tungstate (Bi_2WO_6) varies between 5 and

RSC Advances Accepted Manuscript

10% in weight. Hence, even using 1/20 and 1/10 the amount of 8 mg of non-entrapped Bi_2WO_6 used in previous work,[4] the conversion of glycerol over silica-entrapped Bi_2WO_6(1) and Bi_2WO_6(2) proceeds up to 41% and 58%, respectively, under visible light irradiation for 10 h.

Table 1. Photocatalytic selective oxidation of glycerol over non-entrapped Bi_2WO_6 and over silica-entrapped Bi_2WO_6 catalyst under the irradiation of visible light in water[a]

Photocatalyst	Time (h)	Conversion (%) glycerol	Selectivity (%)		
			dihydroxyacetone	glyceraldehyde	others
Bi_2WO_6(1)	2	11	63	28	9
	4	20	62	27	11
	6	28	58	25	17
	8	35	55	24	21
	10	41	53	24	23
non-entrapped Bi_2WO_6(1)	2	3	95	5	0
	4	5	93	7	0
Bi_2WO_6(2)	2	16	97	3	0
	4	29	95	5	0
	6	40	94	5	1
	8	50	92	6	2
	10	58	91	6	3
non-entrapped Bi_2WO_6(2)	2	6	95	5	0
	4	9	93	7	0

[a]Reaction conditions: 0.1 mmol glycerol, 1.5 mL H_2O, T = 25 °C, visible light >420 nm. For purposeful comparison, the amount of non-entrapped Bi_2WO_6 used for photocatalytic oxidation of glycerol is the same as that of Bi_2WO_6 in silica-entrapped Bi_2WO_6 namely 0.8 mg for Bi_2WO_6(2) and 0.4 mg for Bi_2WO_6(1).

A direct comparison of glycerol conversion over 8 mg of silica-entrapped Bi_2WO_6(2) (10% w/w catalytst loading, the photoactive Bi_2WO_6 is 0.8 mg) and 0.8 mg of non-entrapped Bi_2WO_6 [Bi_2WO_6(2)] under visible light irradiation of 4 h clearly shows that the photoactivity for glycerol conversion over silica-entrapped Bi_2WO_6(2) is indeed greatly enhanced. That is, under visible light irradiation for 4 h using one tenth the amount of non-entrapped Bi_2WO_6, the conversion of glycerol reaches 29%, which is more than 3 times higher than that over non-entrapped Bi_2WO_6.[4]

In addition, it is worth noting that the catalyst of higher loading Bi_2WO_6(2) retains the original high selectivity to DHA of the non-entrapped Bi_2WO_6 photocatalyst.[3] However, this is not the case for the silica-entrapped catalyst Bi_2WO_6(1) with lower loading of Bi_2WO_6. This means that the loading amount of bismuth wolframate entrapped within silica alters not only the photoactivity *but* also the selectivity of the entrapped catalyst (see below for our tentative explanation of this finding).

The XRD patterns in **Figure 1** show that crystalline, well characterized Bi_2WO_6 crystals are encapsulated within the silica xerogels in both cases of 5% w/w and 10% w/w catalyst loading, suggesting that the silica encapsulation does not destroy the crystalline phase structure of Bi_2WO_6 (JCPDS No.73-1126).

The SEM pictures of the silica-entrapped Bi_2WO_6 samples, as shown in **Figure 2**, suggest that, due to the encapsulation of silica, the flower-like structure of non-entrapped Bi_2WO_6 cannot be directly observed. In its place, matrix particles made of

RSC Advances Accepted Manuscript

amorphous silica are clearly observed. The ground granules obtained from grinding a sol-gel monolith, furthermore, have the irregular shape, angular geometry and multiple cracks, which are typical of silica xerogel particles.[10]

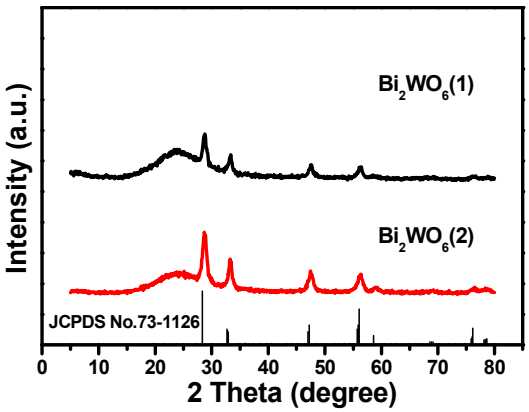

Figure 1. XRD patterns of the samples of silica-entrapped Bi_2WO_6.

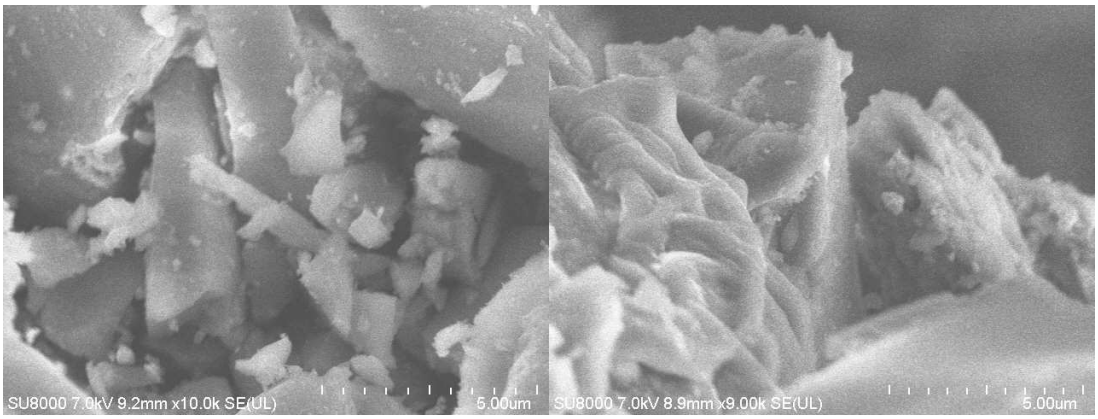

Figure 2 Typical SEM pictures of the samples of silica-entrapped Bi_2WO_6(1) (left) and Bi_2WO_6(2) (right).

RSC Advances Accepted Manuscript

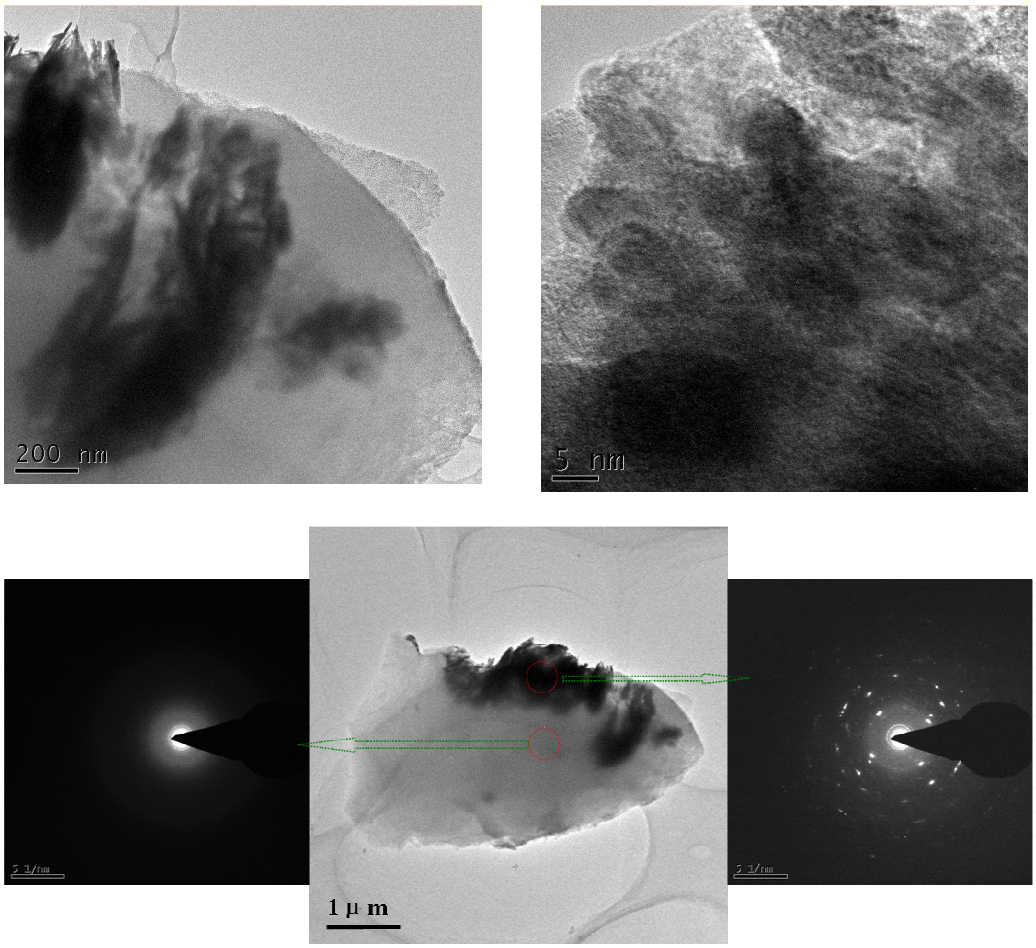

Figure 3 Top: TEM pictures of the samples of silica-entrapped Bi_2WO_6(2). Bottom: images showing the outcome of electron diffraction of different sample regions.

Figure 3 shows the TEM images of sol-gel entrapped Bi_2WO_6(2) sample. It can be seen that, during the entrapping process, the flowerlike superstructure of original Bi_2WO_6 is destroyed. However, the basic unit comprising superstructure of flowerlike Bi_2WO_6 is still retained.[3] Also, the silica encapsulating shell for sol-gel entrapped Bi_2WO_6(2) sample can be clearly distinguished. The bottom image shows the outcome of electron diffraction of regions, from which it is seen that the crystalline structure of Bi_2WO_6 is clearly retained upon the sol-gel encapsulation, where the sol-gel silica shows its amorphous nature.

The optical properties, as reflected by he UV-visible diffuse reflectance spectra (DRS) of the samples of two entrapped catalysts in **Figure 4**, clearly show that the materials can be band-gap-photoexcited by visible light irradiation, but at different extent because of their difference in optical absorption. As expected, due to the higher loading of photoactive Bi_2WO_6 for silica-entrapped Bi_2WO_6(2), the latter catalyst sample has stronger light absorption intensity than Bi_2WO_6(1) in both the UV and visible light regions.

The photoluminescence (PL) spectra are often employed to study surface processes involving the electron-hole fate of the semiconductor. Following the electron-hole pairs

RSC Advances Accepted Manuscript

recombination after a photocatalyst is irradiated, photons are emitted, which results in PL signal. As shown in **Figure 5**, the PL intensity obtained over silica-entrapped Bi_2WO_6(2) is clearly weaker than that of Bi_2WO_6(1), thus suggesting the longer lifetime of photogenerated charge carriers. Thus, the presence of different amounts of SiO_2 affects the PL intensity for SiO_2-entrapped Bi_2WO_6, thereby contributing to the photoactivity difference between two different samples, *i.e.*, silica-entrapped Bi_2WO_6(1) and silica-entrapped Bi_2WO_6(2).

Notably, the photoluminescence (PL) spectra in **Figure 5** clearly show that: (*i*) the PL intensity of silica-entrapped Bi_2WO_6 is much lower than that of non-entrapped Bi_2WO_6, indicating that the sol-gel silica encapsulation contributes to the improved separation of photogenerated electron-hole pairs of Bi_2WO_6 under visible light irradiation; (*ii*) the confinement of Bi_2WO_6 nanocrystals resulting from sol-gel silica encapsulation leads to the significantly different PL emission profiles, suggesting that the synergistic interaction between silica and Bi_2WO_6 influences the spatial transfer kinetics (in addition to improving the lifetime of photogenerated electron-hole pairs).

Together, these factors already mentioned above may account for the difference in both photoactivity and selectivity in the aerobic oxidation of glycerol over silica-entrapped Bi_2WO_6 with different amounts of silica and non-entrapped Bi_2WO_6. Under visible light irradiation, holes and electrons generated inside the Bi_2WO_6 crystalline phase diffuse to the surface of the inner porosity of the silica cages, where they can react with the incoming organic molecules. In brief, the combined effects of semiconductor confinement in the silica cages[6,8-10] and synergistic interaction of Bi_2WO_6 with the SiO_2 cage play a crucial role in affecting the selectivity and activity for oxidation of glycerol.

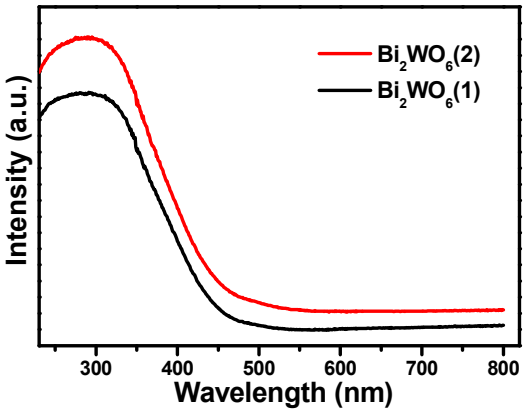

Figure 4. The UV-visible diffuse reflectance spectra (DRS) of the samples of silica-entrapped Bi_2WO_6.

RSC Advances Accepted Manuscript

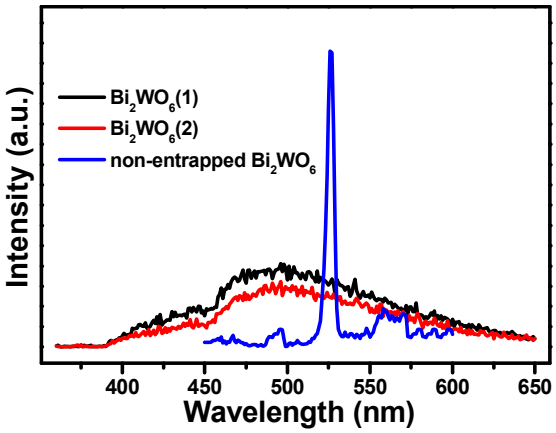

Figure 5. The photoluminescence (PL) spectra of the samples of silica-entrapped Bi_2WO_6 and non-entrapped Bi_2WO_6 with an excitation wavelength of 340 nm.

Table 2 shows the data based on the analysis of N_2 adsorption-desorption isotherms of silica-entrapped catalyst $Bi_2WO_6(1)$ and $Bi_2WO_6(2)$, and non-entrapped Bi_2WO_6. $Bi_2WO_6(1)$ has huge specific surface area (*ca.* 964 m^2/g) along with significant specific pore volume (*ca.* 0.56 cm^3/g). For the higher loading sample, *i.e.*, silica-entrapped $Bi_2WO_6(2)$, the surface area is reduced to *ca.* 517 m^2/g and the pore volume is *ca.* 0.30 cm^3/g. Comparison to non-entrapped Bi_2WO_6, with low surface area of *ca.* 31 m^2/g and pore volume of *ca.* 0.16 cm^3/g, clearly shows that the sol-gel entrapment significantly increases the surface area of the samples.

Table 2. Textural properties of non-entrapped Bi_2WO_6, silica-entrapped $Bi_2WO_6(1)$ and $Bi_2WO_6(2)$ based on the N_2 adsorption-desorption isotherms.

Sample	S_{BET} (m^2/g)	Total pore volume (cm^3/g)	Average pore size (nm)
non-entrapped Bi_2WO_6	31	0.16	5 and 42
$Bi_2WO_6(1)$	964	0.56	2
Bi2WO6(2)	517	0.30	2

Adsorption experiments in the dark shown in **Figure 6** indeed confirm that samples of silica-entrapped Bi_2WO_6 have enhanced adsorption capacity toward glycerol as compared to the non-entrapped Bi_2WO_6.[4] Such an enhanced adsorption capacity reminds one that glycerol can be easily adsorbed and concentrated at the surface of the silica sol-gel cages, with their numerous silanol groups. The very same cages entrap the photocatalytic crystallites and act as chemical sponges that adsorb and concentrate reactants at their surface.[11] The adsorbed glycerol molecules further react at the surface of entrapped Bi_2WO_6 to be oxidized by the positive holes to form the corresponding intermediate, which further reacts with oxygen or activated oxygen to produce DHA and other related products.[4]

RSC Advances Accepted Manuscript

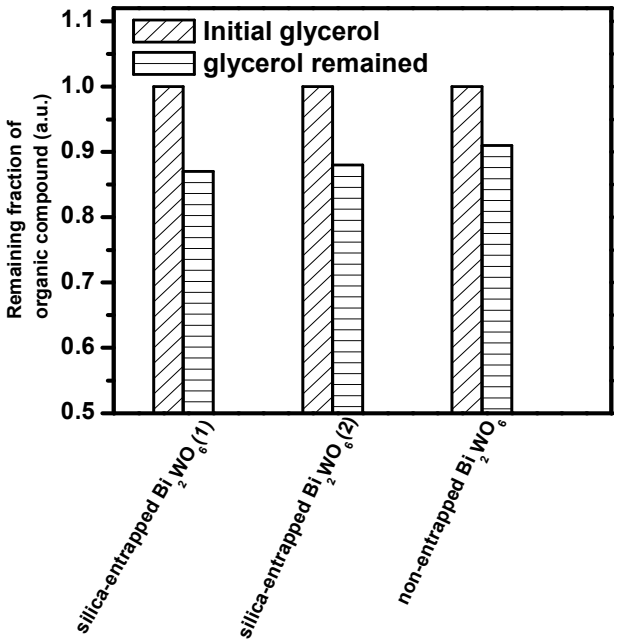

Figure 6. Remaining fraction of glycerol after the adsorption-desorption equilibrium in the dark over silica-entrapped Bi_2WO_6(1), silica-entrapped Bi_2WO_6(2), and non-entrapped flower-like Bi_2WO_6.

However, it should be noted that the surface area is not the only factor that determines the overall photoactivity and selectivity in the photocatalytic oxidation of glycerol. The sample of silica-entrapped Bi_2WO_6(1) has much higher surface area and pore volume than silica-entrapped catalyst Bi_2WO_6(2). But the photoactivity of Bi_2WO_6(1) is lower than Bi_2WO_6(2). This can be attributed to the higher amount loading of photoactive Bi_2WO_6 photoactive species in the silica-entrapped Bi_2WO_6(2), which has a higher visible light absorption capacity and longer lifetime of photogenerated electron-hole pairs, that are the crucial factors determining the overall efficiency of photocatalytic process.

In addition, as discussed above, with the variation of loading amount of photoactive Bi_2WO_6 ingredients in the silica matrix, the selectivity is also affected, suggesting that a synergy interaction between the silica matrix and photoactive Bi_2WO_6 exists in the silica-entrapped Bi_2WO_6 photocatalysts. Silanols at the surface of the sol-gel silica cages favour adsorption of glycerol, enhancing its local concentration and thus easing its reaction with photogenerated active charge carriers including activated molecular oxygen at the cage surface. However, when an insufficient amount of photoactive Bi_2WO_6 is encapsulated, the glycerol molecules are preferentially adsorbed through their more reactive and less hindered primary hydroxyl groups, thereby affording considerable formation of glyceraldehyde (**Table 1**). In contrast, when a sufficient amount of encapsulated Bi_2WO_6 is available for reactivity at the sol-gel cages, glycerol is again preferentially oxidised at the secondary OH group, showing the remarkable effect of both the encapsulating silica matrix and loading of photoactive Bi_2WO_6 species on selectivity toward selective photocatalytic oxidation of glycerol. This effect, we argue, is due to the templating action of the dopant species during the sol-gel hydrolytic polycondensation, in which the dopant species dictate the size and the shape of the encapsulating silica cage in the final xerogel.[12]

In conclusion, we have shown that the sol-gel encapsulation of flower-like Bi_2WO_6 microparticles in SiO_2 xerogels leads to the formation of excellent visible-light-driven

RSC Advances Accepted Manuscript

photocatalytic materials with great potential to act as solar energy transfer materials. The transparent, stabilizing and high surface area of the encapsulated silica matrix allows light penetration, promoting the efficiency of the photogenerated electron-hole separation and enhancing adsorption capacity toward glycerol. As a result, the photoactivity in the aerobic selective oxidation of glycerol under visible light irradiation over silica-entrapped Bi_2WO_6 is greatly enhanced. The synergy between the silica matrix and photoactive entrapped Bi_2WO_6 allows the tunable control of both activity and selectivity for photocatalytic oxidation of glycerol under visible light irradiation.

Glycerol demonstrated herein is just one example of a biomass-derived chemical suitable for chemical upgrade.[12-14] Many other biomass molecules could react, including organic molecules that are not water soluble, and be readily converted to value-added fine chemicals using this SiO_2 xerogels trapped semiconductor composite photocatalyst. Further work is in progress to expand the scope of this simple and feasible method.

Acknowledgements

This article is dedicated to University of Palermo's Professor Giuseppe Aiello for his excellent teaching of physics at chemistry students spanning his lifetime career. We thank PhD student Piera Demma Carà for preparing the catalysts. The support by the NSFC (21173045, 20903023), the Award Program for Minjiang Scholar Professorship, the NSF of Fujian Province for Distinguished Young Investigator Grant (2012J06003), and Program for Returned High-Level Overseas Chinese Scholars of Fujian Province is gratefully acknowledged.

Experimental Section

The catalyst hydrothermal sol-gel synthesis starts from flower-like Bi_2WO_6 prepared following the published procedure.[3] In detail, the simple hydrothermal synthesis starts with sonication of $Bi(NO_3)•5H_2O$ (0.98 g) in 40 mL of 0.3 M HNO_3 aqueous solution. Then, 20 mL of 0.05 M $Na_2WO_4•2H_2O$ solution was added with vigorous stirring and a white precipitate was formed. Subsequently, a NaOH solution (20 mL, 0.2 M) was added under stirring, mixing the resulting solution for 24 h. This mixture was then transferred to a 100 mL Parr autoclave and maintained at 160 °C for 8 h. The resulting sample was recovered by filtration, washed by water, and fully dried at 60 °C in oven to get the final flower-like Bi_2WO_6 samples.

Two sol-gel entrapped catalysts were prepared using TEOS (tetraethylorthosilicate, $Si(OCH_3)_4$) as silica precursor. In one typical preparation, 150 mg of flower-like Bi_2WO_6 was suspended in 1 mL H_2O and the suspension was kept stirring for 30 minutes. The required amount of TEOS (0.025 mol for the 10 wt% catalyst and 0.05 mol for the 5 wt% catalyst) was added to an aqueous solution of HCl 0.05 N and stirred for 30 minutes. After this pre-hydrolysis step, the suspension of Bi_2WO_6 was added and the resulting mixture was kept under mechanical stirring for 30 minutes, after which an aliquot of NaOH 1 N (0.1 mL for 10 wt% and 0.18 mL for 5 wt%) was added. Gelification rapidly occurred.

The resulting alcogel was left in a closed vessel for 24 h after which the vessel was opened and left for 3 days at room temperature and pressure (ambient conditions). The doped silica glass monolith thereby obtained was mildly powdered in a mortar and used as such. The sol-gel encapsulated catalyst sample Bi_2WO_6(1) has a 5% w/w catalyst loading, and Bi_2WO_6(2) has a 10% w/w catalytst loading. To check the materials synthesis reproducibility, similar catalysts (not shown) were prepared also in China using the same methodology. Almost identical results were obtained both for the

RSC Advances Accepted Manuscript

materials and their synthetic application, confirming full reproducibility of both sol-gel materials synthesis and hydrothermal synthesis of flower-like Bi_2WO_6.

The morphology information was determined by a field-emission scanning electron microscope (FESEM, FEI Nova NANOSEM 230). Transmission electron microscopy (TEM) images were collected using a JEOL model JEM 2010 EX microscope at an accelerating voltage of 200 kV. The crystalline structure of the catalysts was determined by powder X-ray diffraction (XRD), using Ni-filtered Cu Kα radiation in the 2θ range from 5° to 80° with a scan rate of 0.08° per second. The optical properties of the catalysts were analyzed by UV-vis diffuse reflectance spectroscopy (DRS) using a Cary-500 spectrophotometer over a wavelength range of 200-800 nm, during which $BaSO_4$ was employed as the internal reflectance standard. Nitrogen adsorption-desorption isotherms and the Brunauer-Emmett-Teller (BET) surface area were collected at 77K using Micromeritics ASAP 2010 equipment. The photoluminescence (PL) spectra were measured on an Edinburgh FL/FS900 spectrophotometer. For the PL analysis of solid samples of Bi_2WO_6, the excitation wavelength is 340 nm. The PL spectra are often employed to study surface processes involving the electron-hole fate of semiconductor. With the electron-hole pairs recombination after a semiconductor photocatalyst is irradiated, photons are emitted, thus resulting in PL. Thus, the PL analysis reflects the fate of electron-hole pairs photogenerated from semiconductor Bi_2WO_6 encapsulated into the sol-gel silica matrix.

The aerobic oxidation of glycerol in water was carried out in a 10 mL Pyrex glass bottle under the irradiation of visible light using a 300 W Xe arc lamp with a UV cutoff filter (λ>420 nm). In a typical process, a mixture of 8 mg solid catalyst and 0.1 mmol of glycerol were added to 1.5 mL water. The mixture, saturated with pure molecular oxygen from a gas cylinder, was transferred into a 10 mL Pyrex glass bottle and stirred for 10 min. After the reaction, the mixture was centrifuged at 12,000 rpm for 20 minutes to separate and remove the catalyst particles. The remaining solution was analyzed with a Shimadzu Liquid Chromatograph (DGU-20A3, equipped with a 512 Diode Array Detector and a C18 analysis column).

RSC Advances Accepted Manuscript

Table of Contents

Sol-Gel Entrapped Visible Light Photocatalysts for Selective Conversions

Yanhui Zhang, Rosaria Ciriminna, Giovanni Palmisano, Yi-Jun Xu and Mario Pagliaro

A new photoactive, low-cost nanomaterial to harvest solar energy and use it a selective reactant is now available. Sol-gel encapsulation of flower-like Bi_2WO_6 into transparent silica glass affords a catalyst far more active, but still highly selective, compared to the non-entrapped species.

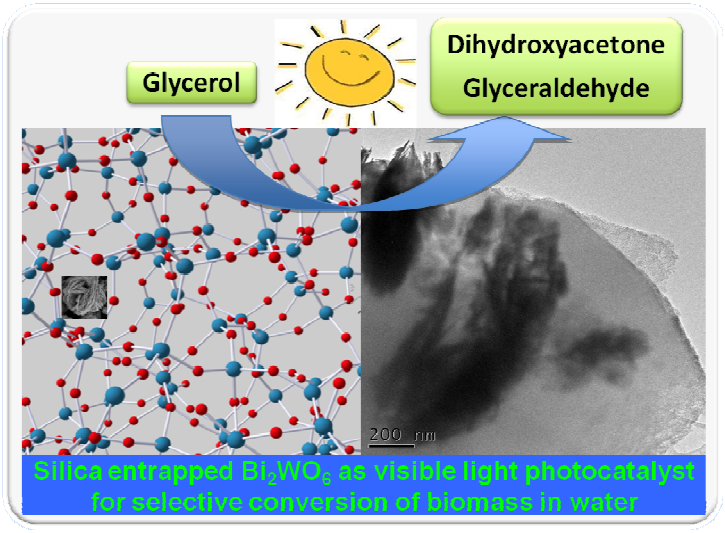

RSC Advances Accepted Manuscript

References

1. V. Augugliaro, V. Loddo, M. Pagliaro, G. Palmisano, L. Palmisano, *Clean by Light Irradiation*, RSC Publishing, Cambridge, UK: 2010.
2. G. Palmisano, V. Augugliaro, M. Pagliaro, L. Palmisano, *Chem. Commun.* **2007**, 3425.
3 . M. Cherevatskaya, S. Füldner, C. Harlander, M. Neumann, S. Kümmel, S. Dankesreiter, A. Pfitzner, K. Zeitler, B. König, *Angew. Chem. Int. Ed.* **2012**, *51*, 4062.
4. Y. Zhang, N. Zhang, Z.-R. Tang, Y.-J. Xu, *Chem. Sci.* **2013**, *4*, 1820.
5. C.-H. Zhou, X. Xia, C.-X. Lin, D.-S. Tong, J. Beltramini, *Chem. Soc. Rev.* **2011**, *40*, 5588.
6. M. Pagliaro, R. Ciriminna, G. Palmisano, *Chem. Soc. Rev.* **2007**, *36*, 932.
7. a) A. Slama-Schwok, D. Avnir, M. Ottolenghi, *Photochem. Photobiol.* **1991**, *54*, 525; b) B. Dunn, J. Zink, *J. Mater. Chem.* **1991**, *1*, 903.
8. A. Molinari, A. Maldotti, A. Bratovcic, G. Magnacca, *Catal. Today* **2013**, *206*, 46.
9. S. Farhadi, Z. Babazadeh, M. Maleki, *Acta Chim. Slov.* **2006**, *53*, 72.
10. R. Ciriminna, A. Fidalgo, F. Béland, V. Pandarus, L. M. Ilharco, M. Pagliaro, *Chem. Rev.* **2013**, *113*, 6592.
11. D. Avnir, *Acc. Chem. Res.* **1995**, *28*, 328.
12. This effect has been reported for several encapsulated molecules. For example, flavor molecules: a) S. R. Veith, M. Perren, S. E. Pratsinis, *J. Colloid Interface Sci.* **2005**, *283*, 495; and chiral species: b) S. Fireman Shoresh, S. Marx, D. Avnir *Adv. Mater.* **2007**, *19*, 2145.
12. M. Pagliaro, R. Ciriminna, H. Kimura, M. Rossi, C. Della Pina, *Angew. Chem. Int. Ed.* **2007**, *46*, 4434.
13. G. L. Brett, Q. He, C. H. Hammond, P. J. Miedziak, N. Dimitratos, M. Sankar, A. A. Herzing, M. Conte,J. A. Lopez-Sanchez, C. J. Kiely, D. W. Knight, S. H. Taylor, G. J. Hutchings, *Angew. Chem. Int. Ed.* **2011**, *50*, 10136.
14. A. Corma, S. Iborra, A. Velty, *Chem. Rev.* **2007**, *107*, 2411.

RSC Advances Accepted Manuscript